Delayed matrix pencil method for local shear wave viscoelastographic estimation

X Li ‡, S Turco, R M Aarts, H Wijkstra and M Mischi

Department of Electrical Engineering, Eindhoven University of Technology, Eindhoven, The Netherlands

E-mail: x.li1@tue.nl

Abstract. Shear wave (SW) elastography is an ultrasound imaging modality that provides quantitative viscoelastic measurements of tissue. The phase difference method allows for local estimation of viscoelasticity by computing the dispersion curve using phases from two laterally-spaced pixels. However, this method is sensitive to measurement noise in the estimated SW particle velocities. Hence, we propose the delayed matrix pencil method to investigate this problem, and validated it both *in-silico* and *in-vitro*. The performance was compared with the original phase difference method and other two alternative techniques based on lowpass filtering and discrete wavelet transform denoising. The estimated viscoelastic values are summarized in box plots and followed by statistical analysis. Results from both studies show the proposed method to be more robust to noise with the smallest bias and variation in both elasticity and viscosity.

Keywords: shear wave elastography, viscoelasticity, matrix pencil method

Submitted to: *Computer Methods and Programs in Biomedicine Update*

‡ Postal address: Flux 7.079, 5600 MB Eindhoven, The Netherlands. Tel: +31 3963 5572

29 September, 2023

Dear Dr. Zinger and Dr. Iqbal,

We would like to submit an original research article entitled “Delayed matrix pencil method for local shear wave viscoelastographic estimation” for consideration by Computer Methods and Programs in Biomedicine Update.

Shear wave elastography is an ultrasound imaging modality that is used to provide quantitative measurements of tissue elasticity and viscosity through approaches such as the phase difference method. The estimated viscoelastic properties have the potential to serve as valuable biomarkers for the differentiation of benign and malignant tissue. However, the phase difference method is sensitive to measurement noise. The matrix pencil algorithm has gained recognition in reducing noise in power system applications. In this manuscript, we propose an innovative enhancement to the original matrix pencil algorithm by introducing a delay parameter such that it can be employed to mitigate the impact of measurement noise in the phase difference method.

Previous works generally treat the measurement noise as additive white Gaussian noise. In our manuscript, we assess the robustness of the proposed method via two studies: the *in-silico* study by adding white Gaussian noise to the simulated particle velocity data, and the *in-vitro* study in two customized phantoms. Additionally, we developed two alternative methods based on established denoising approaches to serve as points of comparison with our proposed approach.

The results from both studies consistently demonstrated the superior robustness of our proposed method when measurement noise is present. Specifically, our method exhibits the smallest bias and variation in both elasticity and viscosity. Furthermore, a statistical analysis of the absolute error reveals a significant improvement achieved by our proposed method compared to the original phase difference method. The findings of this study contribute to the enhancement in robustness of the original phase difference method, ultimately leading to more accurate estimates of both elasticity and viscosity.

The proposed method is a computer-based ultrasound solution and has the potential to be applied in clinical practice helping more accurate viscoelastic estimates in shear wave elastography. We believe that these aspects align with the scope of the Computer Methods and Programs in Biomedicine Update, making it an ideal choice for submission.

We confirm that this work is original and has not been published elsewhere, nor is it currently under consideration for publication elsewhere.

Thank you for your consideration of this manuscript and we look forward to hearing from you.

Yours sincerely,

Xueting Li

E-mail: x.li1@tue.nl

Affiliation: Eindhoven University of Technology

Delayed matrix pencil method for local shear wave viscoelastographic estimation

X Li ‡, S Turco, R M Aarts, H Wijkstra and M Mischi

Department of Electrical Engineering, Eindhoven University of Technology, Eindhoven, The Netherlands

E-mail: x.li1@tue.nl

Abstract. Shear wave (SW) elastography is an ultrasound imaging modality that provides quantitative viscoelastic measurements of tissue. The phase difference method allows for local estimation of viscoelasticity by computing the dispersion curve using phases from two laterally-spaced pixels. However, this method is sensitive to measurement noise in the estimated SW particle velocities. Hence, we propose the delayed matrix pencil method to investigate this problem, and validated it both *in-silico* and *in-vitro*. The performance was compared with the original phase difference method and other two alternative techniques based on lowpass filtering and discrete wavelet transform denoising. The estimated viscoelastic values are summarized in box plots and followed by statistical analysis. Results from both studies show the proposed method to be more robust to noise with the smallest bias and variation in both elasticity and viscosity.

Keywords: shear wave elastography, viscoelasticity, matrix pencil method

Submitted to: *Computer Methods and Programs in Biomedicine Update*

‡ Postal address: Flux 7.079, 5600 MB Eindhoven, The Netherlands. Tel: +31 3963 5572

1. Introduction

Shear wave (SW) elastography is widely used in many clinical applications to provide quantitative measurements of the mechanical properties of tissue (Mitri et al. 2010, Chen et al. 2013, Wang & Insana 2013, Wood et al. 2019, Trutna et al. 2020). By using a focused ultrasound push pulse to induce an acoustic radiation force (ARF), local tissue motion in the axial direction is generated. Such motion forms SWs propagating through the surrounding tissues in the lateral direction, which are tracked using ultrasound imaging. The tissue velocity in the axial direction is referred to as SW particle velocity.

Changes in the mechanical properties of soft tissues are often associated with the presence of disease. For example, it was found that the mean hepatic elasticity is higher in higher stages of fibrosis, and the mean viscosity is significantly higher in patients with cirrhosis than in control (Huwart et al. 2006). The standard method to estimate elasticity and viscosity is based on the k-space analysis of SW particle velocities (Rouze et al. 2015), where an averaged viscoelastic map of the region of interest (ROI) can be deduced.

However, a more local viscoelasticity measurement is often relevant in clinical practice; therefore, the phase difference method was introduced (Chen et al. 2009). In this method, the phase difference of SWs measured at two adjacent pixels is estimated through their temporal Fourier transform (FT), to derive a phase velocity dispersion curve, which is then interpreted by fitting an appropriate rheological model.

While allowing for a local assessment of viscoelasticity, the phase difference method is sensitive to noise in the estimated SW particle velocities. A well-known noise source is speckle noise, which is caused by stronger speckles, located off the main-beam axis, dominating the estimated particle velocities over weaker on-axis speckles (Elegbe & McAleavey 2013, McAleavey et al. 2015). Speckle noise is closely related to the settings (beamforming) of the ultrasound imaging system (Ersepke et al. 2019, Ahmed & Doyley 2020). However, in this work, we aim at reducing the impact of uncorrelated noise in the measured SW particle velocity signals, which we refer to as measurement noise. This type of noise can be introduced, for example, from electronic sources. In modeling and simulations, the measurement noise is generally treated as additive white Gaussian noise (AWGN) (Langdon et al. 2015, Kijanka & Urban 2021).

To make the phase difference method more robust, we present a signal processing approach based on the matrix pencil (MP) algorithm, which has been widely used in power system applications (Crow & Singh 2005). A time delay is added to the standard MP algorithm to account for the SW arrival time at the measurement pixels, and a singular value decomposition (SVD)-based rank reduction with locally optimized threshold is applied to further improve the signal-to-noise ratio (SNR).

2. Material and methods

2.1. Delayed matrix pencil method

The original MP method is one of the variants of the Prony method, which can be used to extract signal parameters in the presence of noise (Kumaresan et al. 1984). The MP method was shown to be more efficient in computation and less sensitive to AWGN than Prony (Hua & Sarkar 1990, Grant & Crow 2011). Basically, it approximates a sequence of uniformly sampled signal $x[n]$ $(n = 1, 2, ...N)$ by a sum of p exponential functions given as

$$x[n] = \sum_{k=1}^{p} A_k \exp(\mathrm{i}\theta_k) \exp[(\alpha_k + \mathrm{i}2\pi f_k)T_s(n-1)], \tag{1}$$

where the unknown parameters A_k, θ_k, α_k, f_k and T_s are the amplitude, phase, damping factor, frequency and sampling period, respectively.

Time-varying signals are mostly fit well with the original MP method. However, the particle velocity signal exhibits a flat period before the SW arrival at the measurement location. This flat period is not represented by the MP model, resulting in poor fitting. To overcome this problem, we introduce a time delay τ to achieve a better overall fitting of the particle velocities.

In practice, the values of τ and p for each signal are determined using the grid search method. The optimal values τ_d and p_d are the values that minimize the root mean square error between the original signal and the model fit. The lower bound of the searching range for τ is automatically determined at the time instant corresponding to the appearance of the SW, after the flat initial segment indicating no tissue displacement. To do so, a parametric method for global optimization is employed that is able to identify abrupt changes in the standard deviation (SD) of the signal while minimizing the total residual error (Lavielle 2005, Killick et al. 2012). The upper bound of the searching range is automatically determined at the time corresponding to the SW peak. This searching range ensures that the MP fitting starts after the SW appearance time. The searching range of p is between one and half of the signal length, so as to avoid over-fitting.

A moving average (MA) filter is applied to the signal from its beginning to τ_d. The window size of the MA filter is 5 pixels (0.5 ms), as this is the smallest size for which the sum of absolute error (AE) between the original signal and the smoothed signal starts converging based on our experimental data.

The MP fitting is applied on the delayed signal $x_\mathrm{d}[n] = x[n+\tau_\mathrm{d}]$ $(n = 1, 2, ...N-\tau_\mathrm{d})$. Let N_d denote the signal length of $x_\mathrm{d}[n]$. We can write:

$$x_\mathrm{d}[n] = \sum_{k=1}^{p_\mathrm{d}} A_k \exp(\mathrm{i}\theta_k) \exp[(\alpha_k + \mathrm{i}2\pi f_k)T_s(n-1)] \tag{2a}$$

$$= \sum_{k=1}^{p_\mathrm{d}} h_k \cdot z_k^{(n-1)}, \tag{2b}$$

where $h_k = A_k \exp(\mathrm{i}\theta_k)$ are the time-independent components and $z_k = \exp[(\alpha_k + \mathrm{i}2\pi f_k)T_s]$ are the time-dependent components (signal poles).

The signal poles z_k are found by solving a generalized eigenvalue problem (Fernández Rodríguez et al. 2018, Sarrazin et al. 2011). To do so, a Hankel matrix $\mathbf{Y}$,

$$\mathbf{Y} = \begin{bmatrix} x_\mathrm{d}[1] & x_\mathrm{d}[2] & \cdots & x_\mathrm{d}[p_\mathrm{d}+1] \\ x_\mathrm{d}[2] & x_\mathrm{d}[3] & \cdots & x_\mathrm{d}[p_\mathrm{d}+2] \\ \vdots & \vdots & \ddots & \vdots \\ x_\mathrm{d}[N_\mathrm{d}-p_\mathrm{d}] & x_\mathrm{d}[N_\mathrm{d}-p_\mathrm{d}+1] & \cdots & x_\mathrm{d}[N_\mathrm{d}] \end{bmatrix}, \tag{3}$$

is constructed based on the measured signals at each pixel.

To improve the robustness, we decompose $\mathbf{Y}$ by SVD as

$$\mathbf{Y} = \mathbf{U}\mathbf{S}\mathbf{V}^\mathrm{H}, \tag{4}$$

where the superscript H represents the Hermitian transpose; $\mathbf{U}$ and $\mathbf{V}$ are eigenvectors; $\mathbf{S}$ is a diagonal matrix containing the singular values of $\mathbf{Y}$ in a descending order. The corresponding eigenvectors are separated into two groups: the m eigenvectors associated with the signal and the rest of eigenvectors associated with noise. When sorted in decreasing order, the curve of the singular values shows an inflection point where it starts to converge to a constant value. The rank of the Hankel matrix is reduced to the order m corresponding to this inflection point, resulting in effective noise suppression. Thus, the inflection point is determined specifically for each local estimation.

Next, a reduced matrix $\mathbf{V}_\mathrm{r}$ is formed from $\mathbf{V}$ using only the rows corresponding to the m more significant singular values, written as

$$\mathbf{V}_\mathrm{r} = [v_1, v_2, \cdots, v_m]. \tag{5}$$

The following four matrices can then be defined from $\mathbf{V}_r$:

$$\mathbf{V}_1 = [v_1, v_2, v_3, \cdots, v_{m-1}], \tag{6a}$$

$$\mathbf{V}_2 = [v_2, v_3, v_4, \cdots, v_m], \tag{6b}$$

$$\mathbf{Y}_1 = \mathbf{V}_1^\mathrm{H}\mathbf{V}_1, \tag{6c}$$

$$\mathbf{Y}_2 = \mathbf{V}_2^\mathrm{H}\mathbf{V}_1. \tag{6d}$$

The values of z_k are the eigenvalues of the matrix pencil $\mathbf{Y}_2 - \lambda\mathbf{Y}_1$, that is,

$$z_k = eigenvalues(\mathbf{Y}_1^+\mathbf{Y}_2), \tag{7}$$

with $\mathbf{Y}_1^+$ being the Moore-Penrose pseudoinverse of $\mathbf{Y}_1$.

With z_k known, we can find the damping factor α_k and frequency f_k by

$$\alpha_k = \ln|z_k|/T_s, \tag{8}$$

$$f_k = \arctan[\Im(z_k), \Re(z_k)]/(2\pi T_s). \tag{9}$$

Subsequently, we can determine the components h_k by solving

$$\begin{bmatrix} z_1^0 & z_2^0 & \cdots & z_{p_\mathrm{d}}^0 \\ z_1^1 & z_2^1 & \cdots & z_{p_\mathrm{d}}^1 \\ \vdots & \vdots & \ddots & \vdots \\ z_1^{p_\mathrm{d}-1} & z_2^{p_\mathrm{d}-1} & \cdots & z_{p_\mathrm{d}}^{p_\mathrm{d}-1} \end{bmatrix} \begin{bmatrix} h_1 \\ h_2 \\ \vdots \\ h_{p_\mathrm{d}} \end{bmatrix} = \begin{bmatrix} x_\mathrm{d}[1] \\ x_\mathrm{d}[2] \\ \vdots \\ x_\mathrm{d}[p_\mathrm{d}] \end{bmatrix}. \tag{10}$$

The amplitude A_k and phase θ_k can then be derived as

$$A_k = |h_k|, \tag{11}$$

$$\theta_k = \arctan[\Im(h_k), \Re(h_k)]. \tag{12}$$

The arctan denotes the two-argument arctangent function in (9) and (12). Finally, the fit signal is reconstructed using (1). One example of the delayed MP fit signal is shown in Figure 1.

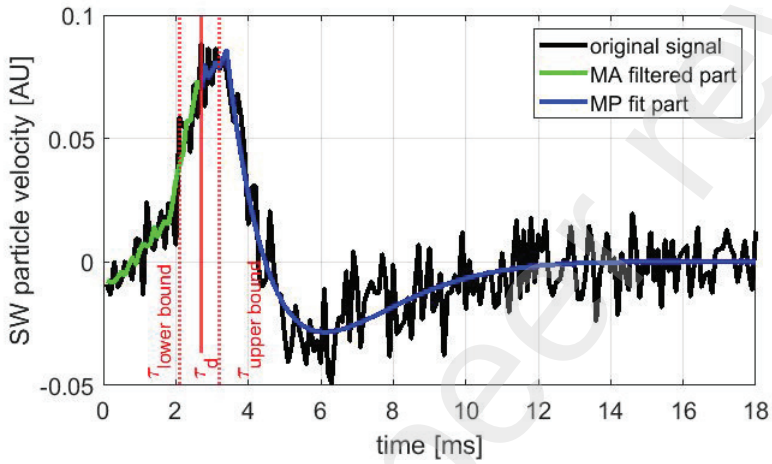

Figure 1. one example of the delayed MP fit signal. The time delay τ_d and the MP order p_d are determined using the grid search method. The lower bound of τ is automatically detected at the SW appearance time; The upper bound of τ is at the signal maximum. The fit signal contains two parts: before τ_d, the signal is processed by MA filtering and after τ_d it is fit by the MP method.

2.2. In-silico study

The proposed method was first tested on simulated data following the analytic solution in (Rouze et al. 2015). The simulated SW particle velocity map in the spatiotemporal domain had a pixel size of 0.1 mm × 0.1 ms. Four groups were simulated with different elasticity and viscosity values, as listed in Table 1. The values of groups A and B were chosen around the reference values of the phantom F1 detailed in the following section. Groups C and D were chosen from the *ex-vivo* prostate viscoelastic values (Mitri et al. 2010). Simulated data were generated with those values based on the Kelvin–Voigt (KV) rheological model. To test the robustness of the proposed method, the simulated particle velocity data were examined by adding AWGN to achieve SNRs of 19 dB and 7 dB (Kijanka & Urban 2021) for 10 noise realizations each.

2.3. In-vitro study

Two customized phantoms (F1 and F2) fabricated by CIRS, Inc. (Norfolk, VA) were used for the *in-vitro* study. The experiment was performed using a Verasonics Vantage

Table 1. Shear Elasticity and viscosity reference values for the *in-silico* study

Group	Shear Elasticity [KPa]	Shear Viscosity [Pa·s]
A	1.5	0.5
B	4.0	1.2
C	7.0	2.0
D	12.8	4.9

256 ultrasound research platform (Kirkland, WA, USA) with an L11-4v linear array transducer. A 1500-cycle push pulse with a center frequency of 4.5 MHz was applied. An ultrafast imaging protocol with a frame rate of 10 kHz was used to track the resulting SWs. The in-phase and quadrature (IQ) data were saved for post-processing. The final pixel dimensions were 0.086 mm in the axial direction and 0.208 mm in the lateral direction. In total, 10 acquisitions under the same conditions were recorded.

The SW particle velocity map at the focal depth was then calculated using the Loupas autocorrelator (Loupas et al. 1995). In our experiment, the axial range N_{ax} and ensemble range N_{ens} were set to be 20 samples and 5 frames, respectively. As the true viscoelastic values of the phantoms are unknown, we evaluated the reference values using the standard k-space method (Rouze et al. 2015) for each acquisition and then averaged. The fitting range was 200-400 Hz, and the resulting elasticity and viscosity of F1 were 1.6 kPa and 1.0 Pa·s, respectively. For F2, they were 7.2 kPa and 2.5 Pa·s, respectively.

2.4. Comparison methods

In both studies, the SW particle velocity signals were first processed with the proposed MP method. For comparison, we also developed two alternative methods based on well-known denoising approaches, which are lowpass filtering and discrete wavelet transform (DWT) denoising. All three methods were compared to the original method, where the particle velocity signals were used without any processing.

For the lowpass filtering method, the particle velocity signals were filtered using a minimum-order finite impulse response (FIR). A FIR filter was chosen due to its stability. The cutoff frequency was set to be the frequency with a 30 dB energy decay with respect to the maximal energy peak of the signal. The value of 30 dB was chosen conservatively for suppressing the noise without distorting the signals.

The DWT-based denoising method contains three steps: forward transformation of signals to the wavelet domain, applying a threshold to the detail coefficients, and inverse transformation to the original domain with the original approximation coefficients and the modified detail coefficients. Here, a Symlet wavelet with 4 vanishing moments (sym4) was used with a posterior median threshold rule. The first three levels were kept for reconstruction, resulting in the reconstructed signals being sufficiently smoothed while avoiding distortion of their shapes.

2.5. Quality metrics

For each method, the temporal FT was carried out on the (processed) SW particle velocity signals from two neighboring locations with the spatial distance $\Delta x = 0.5$ mm. Their phase difference $\Delta\phi(\omega)$ can thus be found with ω denoting the angular frequency. The SW speed as a function of ω (dispersion curve) was then computed by $c_s(\omega) = \omega\Delta x/\Delta\phi(\omega)$. After fitting the KV model to the dispersion curve, the elasticity μ and viscosity η were estimated locally. The fitting range was the same as in the standard k-space method, i.e. 200-400 Hz. One example of this procedure based on a pair of clean signals is presented in Figure 2. Finally, we summarized the local elasticity and viscosity of the ROI in box plots.

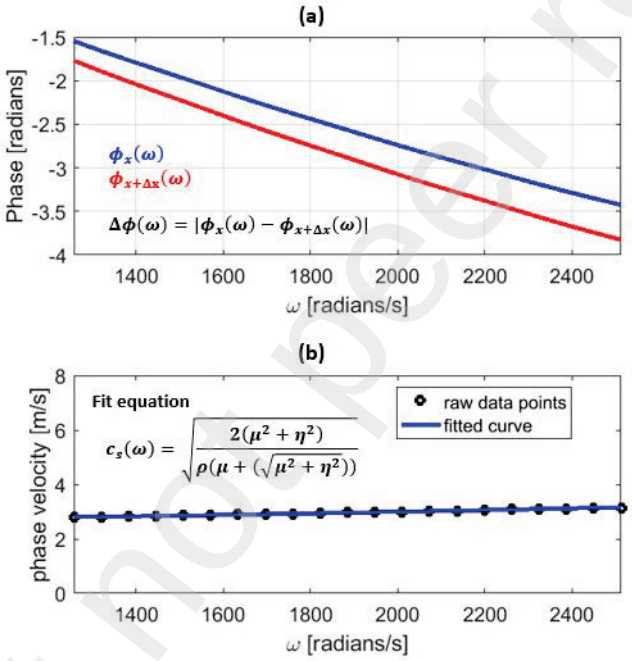

Figure 2. One example to illustrate the phase difference method. (a) Fourier phases of a pair of clean SW particle velocity signals at adjacent locations x and $x + \Delta x$. (b) Phase velocity can be calculated using $c_s(\omega) = \omega\Delta x/\Delta\phi(\omega)$, then the equation shown in (b) based on the KV model is used to fit out elasticity μ and viscosity η. For the original method, phase differences were calculated based on the original SW particle velocity signals; For the other three methods, phase differences were calculated based on the processed signals.

Statistical analysis of the AE was performed in both studies. The Friedman test, followed by a post hoc analysis with the Bonferroni correction, was used to check whether there were significant differences among all methods. Finally, we also characterized the estimated noise in the *in-vitro* study to investigate its distribution.

3. Results

3.1. In-silico study

The simulated SW particle velocity region for the cases of clean data, SNR = 19 dB, and SNR = 7 dB is presented in Figure 3. In Figure 4, we show one example to demonstrate the original SW particle velocity signal and the processed signals using the proposed MP method, the lowpass filtering method and the DWT-based denoising method. For the original method, phase differences were calculated based on the original signals. While for the other three methods, they were calculated based on the processed signals.

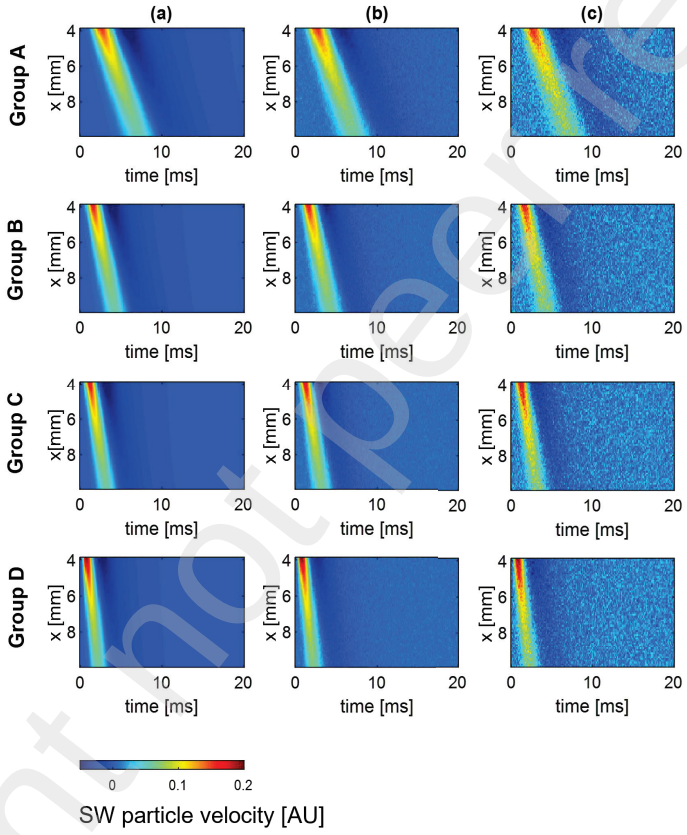

Figure 3. Simulated spatiotemporal SW particle velocity region of four groups. (a) clean data, (b) SNR = 19 dB, and (c) SNR = 7 dB.

The local elasticity and viscosity of the region in Figure 3 were estimated and are summarized as box plots in Figure 5, Figure 6 and Figure 7 for the three cases, respectively. Figure 5 indicates that all four methods have comparable results across all groups for the clean data, with the proposed MP method showing less variation and/or bias in most scenarios. We use the interquartile range as the measure of variation. In both Figure 6 and Figure 7, the MP method gives the most accurate results with the smallest variation and bias for all groups.

The mean and SD of the AE for each group are summarized in Table 2 and Table 3 for the case of SNR = 19 dB and SNR = 7 dB separately. In both tables, the proposed

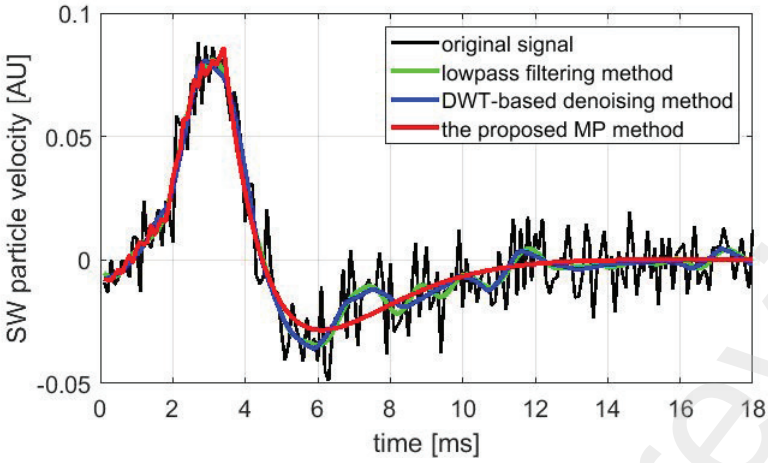

Figure 4. One example to show the original SW particle velocity signal and the processed signals. The black curve is one SW particle velocity signal taken from the Group B with SNR = 7 dB. The green and blue curves are the signals processed by the lowpass filtering method and the DWT-based denoising method, respectively. The red curve is the fit signal with the proposed MP method.

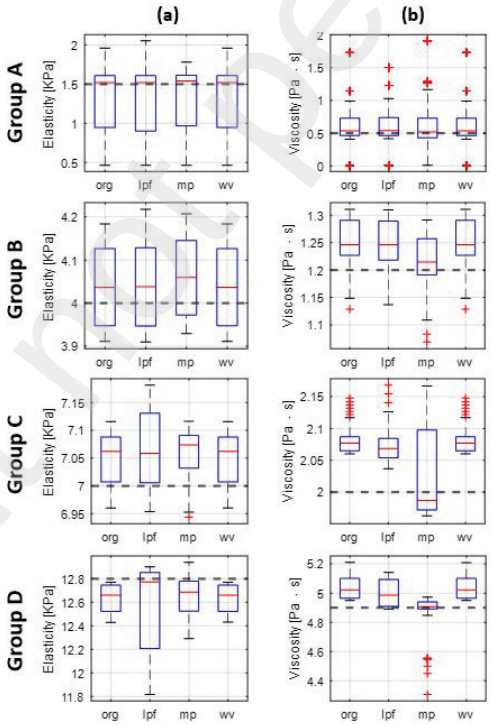

Figure 5. Box plots of local (a) elasticity and (b) viscosity calculated from the simulated region with clean data. Black dashed lines represent the true values. "org", "lpf", "mp" and "wv" represent the original phase difference method, the lowpass filtering method, the proposed MP method, and the DWT-based denoising method, respectively.

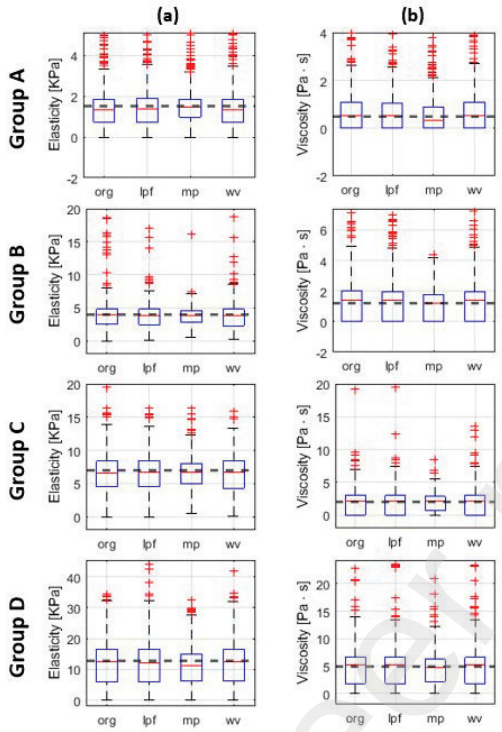

Figure 6. Box plots of local (a) elasticity and (b) viscosity calculated from the simulated region with SNR = 19 dB. Black dashed lines represent the true values. "org", "lpf", "mp" and "wv" represent the original phase difference method, the lowpass filtering method, the proposed MP method, and the DWT-based denoising method, respectively.

Table 2. Mean ± SD of the AE with SNR = 19 dB

	Group	org	lpf	mp	wv
	A	1.44 ± 4.79	1.23 ± 3.61	0.96 ± 2.37	1.37 ± 4.53
Elasticity	B	1.77 ± 3.51	1.65 ± 3.19	1.23 ± 1.83	1.69 ± 3.34
[kPa]	C	2.55 ± 4.02	2.33 ± 1.98	2.02 ± 1.80	2.35 ± 2.14
	D	5.78 ± 4.49	5.80 ± 4.80	5.12 ± 3.79	5.73 ± 4.67
	A	1.77 ± 6.09	1.73 ± 5.69	1.72 ± 5.86	1.66 ± 5.09
Viscosity	B	1.95 ± 5.40	1.81 ± 5.82	0.92 ± 3.33	1.53 ± 4.00
[Pa·s]	C	1.40 ± 1.89	1.53 ± 3.03	1.17 ± 1.55	1.62 ± 3.58
	D	3.29 ± 5.16	3.28 ± 5.34	2.77 ± 4.68	3.32 ± 4.98

MP method shows the lowest mean and SD values compared to the other three methods. For both cases, compared to estimating elasticity and viscosity without pre-processing, the improvement by the proposed MP method is more obvious in the viscosity estimates. For the case of SNR = 19 dB, the AE mean and SD decrease the most by 52.82% and 38.33%, respectively; for the case of SNR = 7 dB, they decrease the most by 55.77% and 36.35%, respectively.

The results of our statistical analysis on the AE of all groups are presented in Figure 8, where the proposed MP method shows a significant difference (p-value <

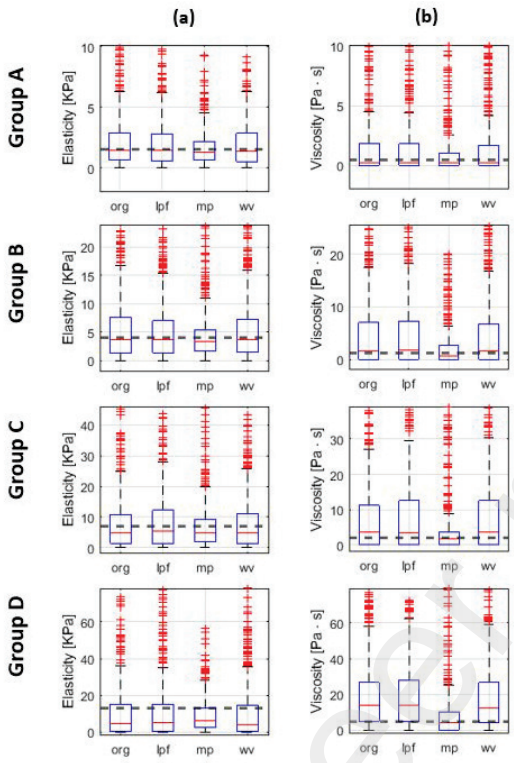

Figure 7. Box plots of local (a) elasticity and (b) viscosity calculated from the simulated region with SNR = 7 dB. Black dashed lines represent the true values. "org", "lpf", "mp" and "wv" represent the original phase difference method, the lowpass filtering method, the proposed MP method, and the DWT-based denoising method, respectively.

Table 3. Mean ± SD of the AE with SNR = 7 dB

	Group	org	lpf	mp	wv
	A	2.62 ± 5.69	2.71 ± 6.58	1.97 ± 5.16	2.43 ± 5.38
Elasticity	B	5.03 ± 7.15	4.77 ± 7.63	3.76 ± 7.36	5.00 ± 7.99
[kPa]	C	7.14 ± 8.81	7.34 ± 8.50	5.14 ± 5.70	6.98 ± 8.19
	D	10.91 ± 8.29	11.27 ± 9.18	8.59 ± 5.36	11.29 ± 8.68
	A	3.50 ± 9.64	3.05 ± 8.13	2.53 ± 8.43	3.24 ± 8.39
Viscosity	B	6.45 ± 11.82	6.25 ± 11.18	3.89 ± 9.85	5.88 ± 10.96
[Pa·s]	C	8.49 ± 13.32	9.50 ± 14.92	3.91 ± 8.31	9.61 ± 15.45
	D	15.76 ± 16.48	15.65 ± 15.88	6.97 ± 10.49	15.44 ± 16.39

0.05) compared with the other three methods.

3.2. In-vitro study

Figure 9(a) presents one measured particle velocity map of the phantom F1; the remaining nine maps are similar. The local elasticity and viscosity of this region were calculated and are shown in Figure 9(b) and Figure 9(c), where the proposed MP method

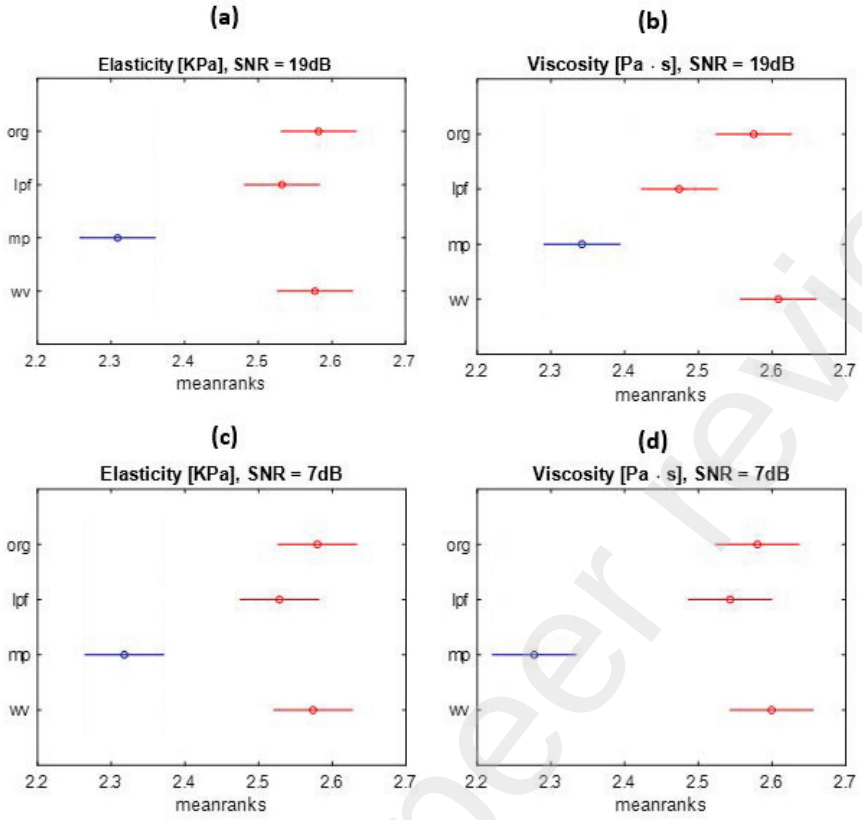

Figure 8. Post hoc analysis of four methods in the *in-silico* study; the results from the proposed method are presented in blue; the results from methods with significant differences compared to the proposed method are presented in red. The circles and bars represent the mean ranks and confidence intervals. (a) Elasticity of the SNR = 19 dB case, (b) Viscosity of the SNR = 19 dB case, (c) Elasticity of the SNR = 7 dB case, (d) Viscosity of the SNR = 7 dB case. "org", "lpf", "mp" and "wv" represent the original phase difference method, the lowpass filtering method, the proposed MP method, and the DWT-based denoising method, respectively.

shows the smallest variation and bias. Figure 9(d), Figure 9(e) and Figure 9(f) show one measured particle velocity map, local elasticity and viscosity for the phantom F2, respectively. Clear improvement in variation is observed in both elasticity and viscosity results. The mean and SD of the AE are summarized in Table 4, where the proposed MP method shows the lowest error in phantom F1, for both elasticity and viscosity estimates, and the lowest error for viscosity in phantom F2.

Figure 10 shows the statistical analysis results, where the proposed MP method achieved a significant difference (p-value < 0.05) in elasticity. Regarding viscosity, it is significantly different from the original method and the DWT denoising method; it is comparable to the lowpass filtering method, yet with slightly lower mean ranks.

To evaluate the SNR of the *in-vitro* study, we assumed the noise to be additive, and the filtered signals using the proposed MP method to represent the "clean" signals. The calculated mean SNR value from all locations and acquisitions was 8.81 dB for

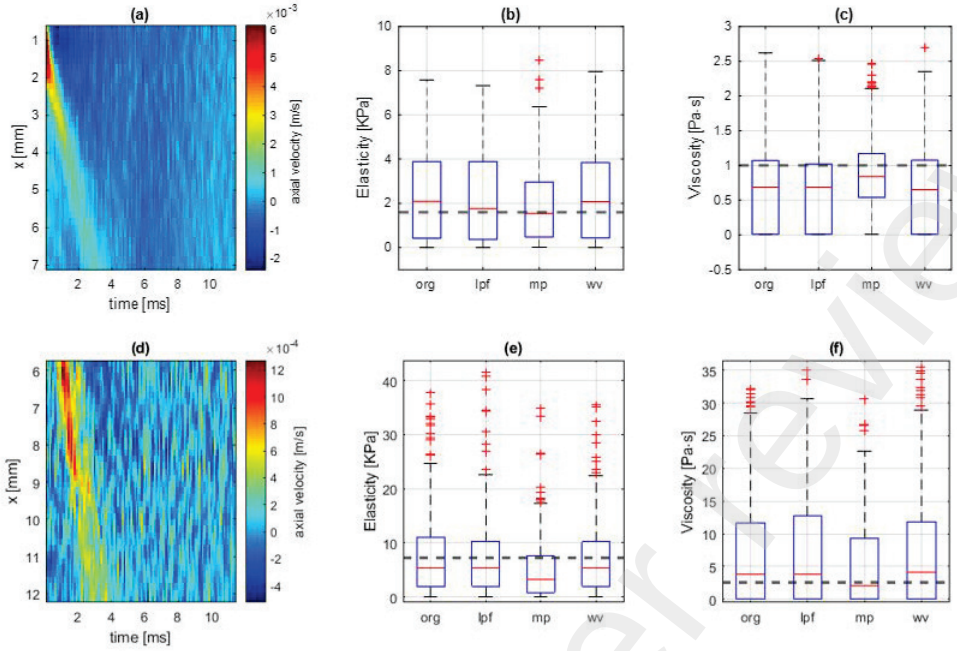

Figure 9. SW particle velocity of one acquisition at the focal depth, (a) phantom F1, (d) phantom F2. Box plots of the calculated local elasticity of 10 acquisitions, (b) phantom F1, (e) phantom F2. Box plots of the calculated local viscosity of 10 acquisitions, (c) phantom F1, (f) phantom F2. Black dashed lines are reference values calculated using the standard k-space method. "org", "lpf", "mp" and "wv" represent the original phase difference method, the lowpass filtering method, the proposed MP method, and the DWT-based denoising method, respectively.

Table 4. Mean ± SD of the AE of the phantoms F1 and F2

	Group	org	lpf	mp	wv
Elasticity	F1	1.80 ± 1.02	1.81 ± 1.06	1.30 ± 1.02	1.82 ± 1.07
[kPa]	F2	9.84 ± 25.42	6.51 ± 10.05	7.99 ± 18.84	7.82 ± 18.38
Viscosity	F1	0.58 ± 0.40	0.59 ± 0.40	0.47 ± 0.35	0.61 ± 0.46
[Pa·s]	F2	8.69 ± 15.21	7.46 ± 12.31	4.93 ± 9.21	8.28 ± 13.52

the phantom F1, which is between the values of 19 dB and 7 dB used in the *in-silico* study. For phantom F2, the calculated mean SNR value was 1.11 dB, which is below 7 dB. The histogram and the power spectrum of noise of the phantom F1 are shown in Figure 11(a) and Figure 11(b), and of the phantom F2 in Figure 11(c) and Figure 11(d), respectively. Notice that the estimated noise has a similar distribution to the AWGN used in simulations. In addition, the Gaussianity of the noise amplitude distribution is confirmed by the Shapiro–Wilk test (p-value = 0.24 and 0.82 for the phantoms F1 and F2 separately).

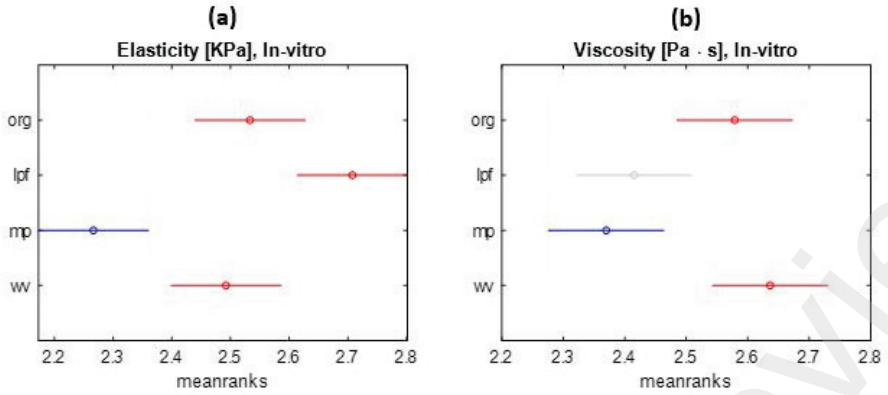

Figure 10. Post hoc analysis of four methods in the *in-vitro* study; the results from the proposed method are presented in blue; the results from methods with significant differences compared to the proposed method are presented in red, without significant differences are shown in gray. The circles and bars represent the mean ranks and confidence intervals. (a) Elasticity, (b) Viscosity. "org", "lpf", "mp" and "wv" represent the original phase difference method, the lowpass filtering method, the proposed MP method, and the DWT-based denoising method, respectively.

4. Discussion

In the standard k-space method, a FT in the spatial domain is required in addition to the FT in the temporal domain. A certain number of spatial points are required to guarantee sufficient frequency resolution for the subsequent estimation. The resulting viscosity and elasticity will then be an averaged value among those points, which limits the spatial resolution of the final viscoelasticity map.

Such limitations in the spatial resolution are overcome in the phase difference method, as it only requires two closely spaced points. The viscosity and elasticity can be evaluated locally per pixel and the spatial resolution only depends on the pixel size. However, the phase difference method is sensitive to noise as noticed when comparing the box plots of the original method in Figure 5, Figure 6 and Figure 7. The phase characteristic of the noisy signals was changed, leading to different dispersion curves, as well as viscoelastic values.

To improve the reliability of the original phase difference method, an approach for accurate and robust phase estimation in noisy signals is sought. The delayed MP method is thus proposed as a robust model-fitting algorithm in the time domain to achieve this. Besides, lowpass filtering and a DWT-based denoising method were implemented for comparison, as the former is a commonly used noise-reduction technique, and the latter is a well-known decomposition-based noise-reduction technique.

Comparing the box plots between the lowpass filtering method and the original method in Figure 5, Figure 6 and Figure 7, no obvious improvements can be seen. Also, no significant difference was observed between these two methods in Figure 8. This is because the employed FIR filter has a linear phase, and the phase difference of the

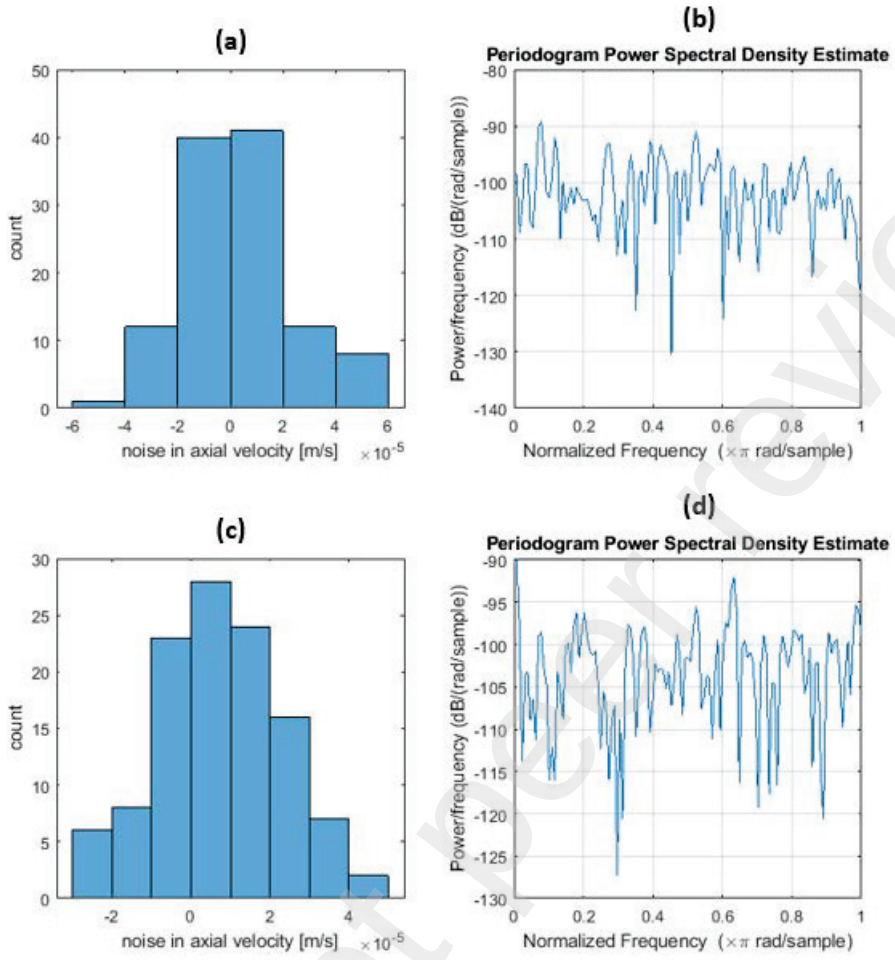

Figure 11. Histogram of the estimated noise amplitude, (a) phantom F1, (c) phantom F2. Power spectrum of estimated noise, (b) phantom F1, (d) phantom F2.

filtered signals is close to that of the noisy signals.

The DWT denoising method decomposes signals using wavelets instead of complex exponential functions as in the MP method. This method attained comparable results to the original method as seen in Figure 5, Figure 6 and Figure 7. The same level of decomposition was kept for SW particle velocities from all locations, which may not be optimal.

On the other hand, the proposed model-fitting-based MP method is more robust to noise. It was demonstrated that using Hankel matrix rank reduction, the MP method can correctly identify the system poles from noisy signals (Almunif et al. 2020). This indicates that the phase difference of the MP-filtered signals can be close to that of clean signals. In addition, we applied an adaptive threshold during the rank reduction, that is, an optimal value is obtained per location automatically. Hence, significant improvements were obtained with the proposed MP method as in Figure 6, Figure 7 and Figure 8.

The results of the *in-vitro* study in Figure 10 confirm these observations, with the

proposed MP method achieving the most significant improvements. The *in-silico* study demonstrates that the MP method is robust to AWGN, and Figure 11 suggests that a similar noise distribution in the *in-vitro* study. Nevertheless, more *in-vitro* experiments should be performed to estimate the noise distribution and to test the robustness of the proposed MP method in the presence of different viscoelastic properties. Furthermore, more investigations can be done to apply localized thresholds for the DWT-based denoising method.

The proposed MP method was applied to SW particle velocity signals measured using the multiple-track-location SW elasticity imaging method. It can also be employed for velocity signals measured from single-track location SW elasticity imaging (SLT-SWEI). STL-SWEI is robust against speckle noise in viscoelasticity estimation while being not immune to other incoherent sources of noise (Ahmed & Doyley 2020). The proposed MP method could facilitate SLT-SWEI by reducing errors from incoherent noise sources; however, this was not explored in this work.

5. Conclusions

A method based on the delayed MP fitting for the estimation of local viscoelasticity from two closely spaced pixels was presented. The proposed method was tested on simulated and *in-vitro* phantom data. In comparison with the original phase difference method, the delayed MP method is more robust to noise. The robustness was tested on signals with AWGN of different SNRs in simulation and the limited *in-vitro* data. Future work will be focused to test this method for data acquired from more *in-vitro* and *in-vivo* studies.

Acknowledgments

Research reported in this work was supported by National Cancer Institute of the National Institutes of Health under award number R01CA252311. The content is solely the responsibility of the authors and does not necessarily represent the official views of the National Institutes of Health.

References

Ahmed, R. & Doyley, M. M. (2020). Parallel receive beamforming improves the performance of focused transmit-based single-track location shear wave elastography, *IEEE transactions on ultrasonics, ferroelectrics, and frequency control* **67**(10): 2057–2068.

Almunif, A., Fan, L. & Miao, Z. (2020). A tutorial on data-driven eigenvalue identification: Prony analysis, matrix pencil, and eigensystem realization algorithm, *International Transactions on Electrical Energy Systems* **30**(4): e12283.

Chen, S., Sanchez, W., Callstrom, M. R., Gorman, B., Lewis, J. T., Sanderson, S. O., Greenleaf, J. F., Xie, H., Shi, Y., Pashley, M. et al. (2013). Assessment of liver viscoelasticity by using shear waves induced by ultrasound radiation force, *Radiology* **266**(3): 964.

Chen, S., Urban, M. W., Pislaru, C., Kinnick, R., Zheng, Y., Yao, A. & Greenleaf, J. F. (2009). Shearwave dispersion ultrasound vibrometry (sduv) for measuring tissue elasticity and viscosity, *IEEE transactions on ultrasonics, ferroelectrics, and frequency control* **56**(1): 55–62.

Crow, M. L. & Singh, A. (2005). The matrix pencil for power system modal extraction, *IEEE Transactions on Power Systems* **20**(1): 501–502.

Elegbe, E. C. & McAleavey, S. A. (2013). Single tracking location methods suppress speckle noise in shear wave velocity estimation, *Ultrasonic imaging* **35**(2): 109–125.

Ersepke, T., Kranemann, T. C. & Schmitz, G. (2019). Quantification of noise in shear wave elasticity imaging caused by speckle, *2019 IEEE International Ultrasonics Symposium (IUS)*, IEEE, pp. 1399–1402.

Fernández Rodríguez, A., de Santiago Rodrigo, L., López Guillén, E., Rodríguez Ascariz, J. M., Miguel Jiménez, J. M. & Boquete, L. (2018). Coding prony's method in matlab and applying it to biomedical signal filtering, *BMC bioinformatics* **19**(1): 1–14.

Grant, L. L. & Crow, M. L. (2011). Comparison of matrix pencil and prony methods for power system modal analysis of noisy signals, *2011 North American Power Symposium*, pp. 1–7.

Hua, Y. & Sarkar, T. K. (1990). Matrix pencil method for estimating parameters of exponentially damped/undamped sinusoids in noise, *IEEE Transactions on Acoustics, Speech, and Signal Processing* **38**(5): 814–824.

Huwart, L., Peeters, F., Sinkus, R., Annet, L., Salameh, N., ter Beek, L. C., Horsmans, Y. & Van Beers, B. E. (2006). Liver fibrosis: non-invasive assessment with mr elastography, *NMR in Biomedicine: An International Journal Devoted to the Development and Application of Magnetic Resonance In vivo* **19**(2): 173–179.

Kijanka, P. & Urban, M. W. (2021). Phase velocity estimation with expanded bandwidth in viscoelastic phantoms and tissues, *IEEE transactions on medical imaging* **40**(5): 1352–1362.

Killick, R., Fearnhead, P. & Eckley, I. A. (2012). Optimal detection of changepoints with a linear computational cost, *Journal of the American Statistical Association* **107**(500): 1590–1598.

Kumaresan, R., Tufts, D. W. & Scharf, L. L. (1984). A prony method for noisy data: Choosing the signal components and selecting the order in exponential signal models, *Proceedings of the IEEE* **72**(2): 230–233.

Langdon, J. H., Elegbe, E. & McAleavey, S. A. (2015). Single tracking location acoustic radiation force impulse viscoelasticity estimation (stl-ve): A method for measuring tissue viscoelastic parameters, *IEEE transactions on ultrasonics, ferroelectrics, and frequency control* **62**(7): 1225–1244.

Lavielle, M. (2005). Using penalized contrasts for the change-point problem, *Signal processing* **85**(8): 1501–1510.

Loupas, T., Powers, J. & Gill, R. W. (1995). An axial velocity estimator for ultrasound blood flow imaging, based on a full evaluation of the doppler equation by means of a two-dimensional autocorrelation approach, *IEEE transactions on ultrasonics, ferroelectrics, and frequency control* **42**(4): 672–688.

McAleavey, S. A., Osapoetra, L. O. & Langdon, J. (2015). Shear wave arrival time estimates correlate with local speckle pattern, *IEEE transactions on ultrasonics, ferroelectrics, and frequency control* **62**(12): 2054–2067.

Mitri, F. G., Urban, M. W., Fatemi, M. & Greenleaf, J. F. (2010). Shear wave dispersion ultrasonic vibrometry for measuring prostate shear stiffness and viscosity: an in vitro pilot study, *IEEE transactions on biomedical engineering* **58**(2): 235–242.

Rouze, N. C., Palmeri, M. L. & Nightingale, K. R. (2015). An analytic, fourier domain description of shear wave propagation in a viscoelastic medium using asymmetric gaussian sources, *The Journal of the Acoustical Society of America* **138**(2): 1012–1022.

Sarrazin, F., Sharaiha, A., Pouliguen, P., Chauveau, J., Collardey, S. & Potier, P. (2011). Comparison between matrix pencil and prony methods applied on noisy antenna responses, *2011 Loughborough Antennas & Propagation Conference*, IEEE, pp. 1–4.

Trutna, C. A., Knight, A. E., Rouze, N. C., Hobson-Webb, L. D., Palmeri, M. L. & Nightingale, K. R. (2020). Viscoelastic characterization in muscle using group speed analysis and volumetric shear wave elasticity imaging, *2020 IEEE International Ultrasonics Symposium (IUS)*, IEEE, pp. 1–4.

Wang, Y. & Insana, M. F. (2013). Viscoelastic properties of rodent mammary tumors using ultrasonic shear-wave imaging, *Ultrasonic imaging* **35**(2): 126–145.

Wood, B. G., Ireson, M. E., Urban, M. W. & Nenadic, I. Z. (2019). Attenuation measuring ultrasound shearwave elastography as a method for evaluating pancreatic viscoelasticity, *Biomedical physics & engineering express* **5**(6): 065016.